Suitability of constitutive models of the structural concrete codes when applied to polyolefin fibre reinforced concrete

A. Enfedaque[1], F. Suárez[2], M. G. Alberti[1], J. C. Gálvez[1]

[1]*Departamento de Ingeniería Civil: Construcción, E.T.S I. de Caminos, Canales y Puertos Universidad Politécnica de Madrid. c/ Profesor Aranguren, s/n, 28040, Madrid*

[2] *Departamento de Ingeniería Mecánica y Minera, Universidad de Jaén, Campus Científico-Tecnológico de Linares, Cinturón Sur, 23700 Linares, Jaén.*

ABSTRACT

The use of fibres as structural reinforcement in concrete is included in standards, providing guidelines to reproduce their behaviour, which have been proven adequate when steel fibres are used. Nevertheless, in recent years new materials, such as polyolefin fibres, have undergone significant development as concrete reinforcement. This work gives insight on how suitable the constitutive models proposed by the Model Code 2010 (MC2010) are in the case of such polymer fibres. A set of numerical models have been carried out to reproduce the material behaviour proposed by the MC2010 and the approach based on the softening function proposed by the authors. The results show that the material behaviour can be reproduced with greater accuracy if the softening function proposed by the authors is employed when this type of macro-polymer fibres is used. Moreover, the relatively complex behaviour of polyolefin fibre reinforced concrete may be reproduced by using such constitutive model.

KEYWORDS: Fibre-reinforced concrete, polyolefin fibres, Model Code 2010, cohesive model

HIGHLIGHTS

- Fracture tests of PFRC are simulated by using several constitutive models
- The use of structural polyolefin fibres should be considered in concrete codes
- Use of a trilinear constitutive model may capture the complex behaviour of PFRC
- Results suggest that the guidelines provided by the standards should be more flexible

1. INTRODUCTION

For some time, the most employed construction material has been concrete and with use being widespread in modern society [1]. Use has been so extensive that consumption of cement has been considered as a reliable parameter to assess the economic activity of countries given that it is directly related to gross domestic product (GDP) [2]. Such extensive use is evidence of several characteristics of the material. Concrete is a material that is easily manufactured, given that the raw materials required are available in almost any location around the world. Water, aggregates, and cement, which is manufactured by subjecting clay and lime to an industrial process, are not only ubiquitous but also relatively inexpensive [3]. The latter characteristic is a key factor in use of concrete as both architectural and civil engineering applications involve remarkable amounts [4, 5]. It is also versatile, as shown in the geometrically complex shapes that concrete elements might take. Another point that cannot be overlooked is that concrete is relatively durable when placed in potentially hazardous areas such as construction sites in marine environments, in mountainous regions and, among others, those that involve tunnels and tunnel linings. In such conditions, concrete of a certain characteristic might provide a prolonged lifespan [6, 7, 8, 9].

None of the aforementioned features would be of any use if concrete did not boast notable mechanical properties. It is commonly known as a material with remarkable compressive strength and modulus of elasticity [10, 11]. Such features, when merged with its adaptability in shaping and reduced cost, enable concrete to be a suitable material in application to structural elements subjected to compressive stresses. Conversely, plain concrete is also known as a quasi-brittle material which is not capable of sustaining high-tensile stresses or boasting visible strains prior to material failure. Consequently, several methods have been developed to detect such strains [12, 13]. This lack of ductility and tensile strength might prevent plain concrete from being used in elements subjected to flexural or tensile stresses such as beams or trusses. However, the combination of plain concrete with steel reinforcing bars, commonly known as reinforced concrete, opens a wide range of uses and applications. Another possible option to improve concrete ductility and, under certain circumstances, its flexural strength would entail adding fibres to the concrete matrix. Short fibres are randomly added to plain concrete during mixing which allows a continuous reinforcement to form. Such material is commonly termed fibre reinforced concrete (FRC). The effect of the addition of fibres in the mechanical properties of concrete depends on numerous parameters, such as the type of fibres used, dosage, shape and size, distribution, orientation and, among others, pull-out response. Several studies have analysed the effect of such parameters on the response of FRC and how, in certain cases, these variables might even modify the fracture surfaces generated when the material fails under tensile stresses [14, 15]. Although several types of fibres have been studied when added to concrete, it should be mentioned that the most used fibre has been the steel one. The properties that steel fibres confer to concrete when forming steel fibre reinforced concrete (SFRC) have enabled use of such a material in a wide range of applications, such as pavements, [16, 17] tunnel linings [18, 19] or even seismic structures [20, 21]. In many of these uses, SFRC is subjected to potentially hazardous environments which might reduce the lifespan of the structural element [22, 23]. This issue has become even more significant in recent decades when an awareness of the total impact of the construction of infrastructure on nature has emerged [24]. One possibility to overcome such durability issues is to use new polymer macro-structural fibres, which are chemically stable when applied in foundations, tunnel linings or marine environments [25, 26, 27, 28]. Polyolefin fibre reinforced concrete (PFRC) is one of the materials available for these uses. Uses of the previously mentioned FRC have been based on extensive research and long-term experience. Nowadays, several national codes and recommendations [29, 30, 31, 32, 33, 34] have set the conditions that a certain FRC should meet so that improvements provided by the fibres added might enable a reduction in the amount of steel reinforcing bars used. Such requirements take into account the residual strength of the FRC studied at certain crack openings which are related to the service limit state (SLS) and the ultimate limit state (ULS). For checking if a FRC formulation boasts sufficient residual strength, laboratory tests are performed that subject FRC specimens to bending tests. Once such tests have been performed, and if the FRC properties exceed the requirements set, the contribution of the fibres might be included in the structural design of the concrete element. Both SFRC and PFRC have been shown as suitable for their application in structural concrete elements [14, 35, 36]. Once such requirements have been checked, the aforementioned recommendations propose several constitutive models that should be applied in the structural design and that have been successfully applied when using SFRC.

The behaviour of PFRC has shown to meet the requirements in the standards although the shapes of the fracture curves have different features compared with those of SFRC [37]. According to the Model Code 2010 (MC2010), the first condition that FRC should meet is a minimum load value, proportional to the maximum strength in the limit of proportionality, at a crack mouth opening displacement of 0.5 mm; this limitation is intended to prevent from a brittle behaviour of the material. Although PFRC with an average fibre dosage might meet the cited requirement, polyolefin fibres need greater deformations to absorb the load that concrete is not capable of sustaining being the first unloading branch steeper than in SFRC. The second condition that MC2010 establishes is that at a crack mouth opening displacement of 2.5 mm the load must be over 20% of the strength at the limit of proportionality. This limitation for PFRC is met even for very low fibre dosages [37]. As there are remarkable differences in the post peak mechanical behaviours of SFRC and PFRC, the applicability of the constitutive models, which are built based on certain values of their residual strength, should be studied. Thus, this study seeks to address the main issues concerning the considerations in the standards of the mechanical behaviour of PFRC.

This contribution supplies additional information for a possible future adaptation of MC2010, and other national concrete structural codes based on it, [38] when applied to PFRC. It is based on modelling three-point bending tests following EN-14651 [37] by using the constitutive relations proposed by MC2010. The numerical analysis has been developed by implementing the rigid-plastic and the linear models proposed in user subroutines into a finite element code. The numerical results of the simulated behaviour of a concrete with four amounts of polyolefin fibres have been compared with the experimental ones. In addition, the results of the simulations by using a trilinear constitutive relation, proposed by the authors in previously published literature, have also been compared with the experimental results. The analysis carried out shows that the best adaptation to the experimental behaviour of PFRC is obtained when the trilinear constitutive function is used. This trend seems to appear when the results of the EN-14651 [37] tests boast a curve defined by three stretches such as the ones obtained in PFRC tests. Moreover, if the rigid-plastic and the linear models proposed by the MC2010 are used some caution should be taken when the SLS of PFRC is studied.

As noted above, current codes on fibre-reinforced concrete, such as MC2010 and other national codes, were developed for steel-fibre reinforced concrete. There are currently other fibres for structural applications, such as polyolefin fibres, whose behaviour does not adapt properly to the constitutive models supplied by concrete codes. This work seeks to explore how fibre-reinforced concrete design models should be adapted to the use of polyolefin fibres, as reinforcement of concrete.

2. POST-PEAK MATERIAL MODELLING

In this section, the numerical modelling of fracture used in the simulations is addressed. In the first part, the embedded cohesive crack model is briefly presented. Since the reader can find a detailed description in previous works published by the authors, this description has been kept to a minimum. In the second part, the model is adapted for PFRC following the guidelines of the MC2010.

2.1 Embedded cohesive crack modelling

Fracture is modelled by means of a cohesive crack model, based on the work proposed by Hillerborg [39] and implemented as an embedded cohesive crack developed in a triangular finite element. This numerical modelling has been used for simulating fracture of concrete [40] and has been adapted for use with brick masonry [41] and, more recently, with PFRC [42].

In this model, fracture is assumed to develop mainly under mode I and with the cohesive stress vector t being parallel to the displacement vector w (thus, it is a central force model), as expressed by (1):

$$t=\frac{f\left(|\tilde{w}|\right)}{|\tilde{w}|}w \; with \; \tilde{w}=max\left(|w|\right) \quad (1)$$

with $f\left(\tilde{w}\right)$ being the softening function, expressed in terms of $\tilde{w}$, which corresponds to an equivalent crack opening that considers the maximum historical opening, necessary for correctly reproducing possible loading-unloading situations.

This formulation is implemented for triangular elements and, as cracks can only develop in lines parallel to the sides of the element, only three cracking orientations are allowed (see Figure 1). It follows a strong discontinuity approach, dividing the element into two parts, A^+ and A^-, with ***t*** being parallel to the crack displacement and constant along the length of the crack L, It is obtained by (2):

$$t=\frac{A}{hL}\sigma\cdot n(2)$$

with A being the area of the element, $h$the height of the triangle over the side opposite to the solitary node and n the unit vector normal to the crack (see Figure 1).

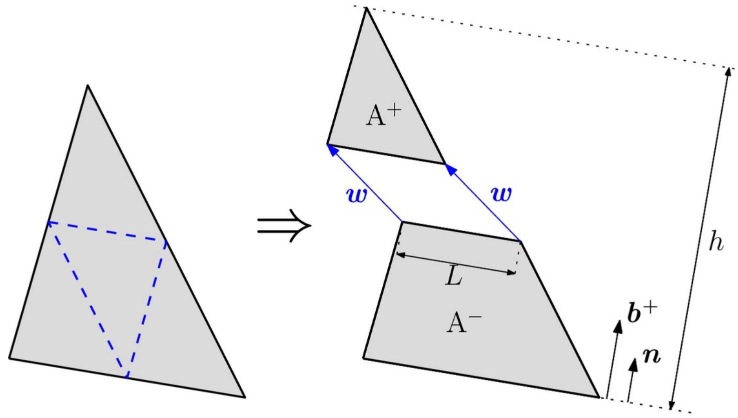

Figure 1: Possible crack paths (left) and geometrical definitions of **w**, **n** and **b**$^+$ (right)

The material around the crack is elastic and the stress tensor is obtained by using a strain vector that results from subtracting the strain due to the crack displacement to the apparent strain ε^a , obtained under elastic considerations and by using the nodal displacements (equation (3)):

$$\sigma=E:¿$$

where E stands for the elastic tangent tensor, $\varepsilon^a$for the apparent strain vector obtained with the nodal displacements, $b^{+¿¿}$ for the gradient vector of the shape function of the solitary node, which can be obtained as:

$$b^{+¿=\frac{1}{h}n(4)¿}$$

Superscript S makes reference to the symmetric part of the tensor, : the usual double -dot product ($(A:B)_{ij}=A_{ijkl}b_{kl}$) and $\otimes$ the usual direct product ($(a\otimes b)_{ij}=a_i b_j$).

Lastly, by using the expression of the stress tensor (3), the stress vector can be obtained as:

$$t=\frac{f(|\tilde{w}|)}{|\tilde{w}|}w=[E:\varepsilon^a]\cdot n-¿$$

This can be rewritten as:

$$¿$$

where 1 identifies the second-order identity tensor.

By using this expression, the crack displacement can be solved for a certain set of nodal displacements by means of the Newton-Raphson method. This model has been implemented by using a user subroutine UMAT of Abaqus® and, since it needs information about the geometry of the model (the nodes coordinates of each element), it reads a previously prepared external file.

2.2 Model adopted by the MC2010

The MC2010 provides two possible constitutive laws to reproduce the behaviour of FRC, with one describing a rigid-plastic behaviour and another one a linear behaviour. These models are defined by parameters that make reference to the values of the residual flexural tensile strength and the crack mouth opening displacement (CMOD) at specific instants during a three-point bending test. In particular, the expression of the residual flexural tensile strength for a specific value of the CMOD may be obtained by expression (7):

$$f_{R,j} = \frac{3 F_j l}{2 b h_{sp}^2} \quad (7)$$

where $f_{R,j}$ is the residual flexural tensile strength in MPa corresponding to a value of the $CMOD = CMOD_j$ in mm, F_j is the load in N applied when $CMOD = CMOD_j$ (in mm), l is the span length, b the specimen width and h_{sp} the height of the notched section (ligament) where the crack propagates, with all these dimensions being in mm (see Figure 2b). Consequently, f_{R1} stands for the residual strength at a CMOD of 0.5mm and f_{R3} stands for the residual strength at a CMOD of 2.5mm. Figure 2a shows a typical load-CMOD curve for FRC where some values of F and CMOD are identified according to the previous description, as described in the MC2010. Expression (7) can be easily obtained by applying the basic principles of the strength of materials at the notched section of the specimen.

a)

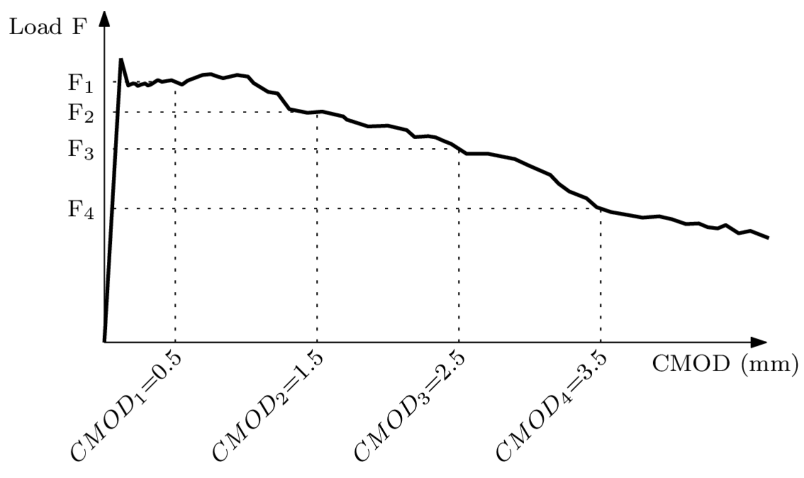

b)

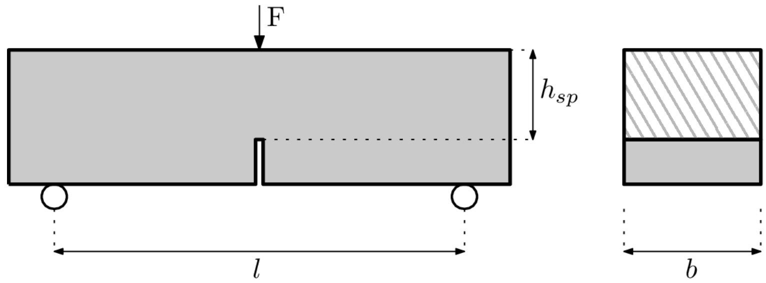

Figure 2: a) Typical load F-CMOD curve for FRC and b) geometry of a three-point bending test specimen.

As mentioned before, MC2010 proposes two possible constitutive laws for FRC. The rigid-plastic model simply describes a constant stress behaviour from the point at which cracking begins ($w=0$) until it reaches a limit value (w_u). In this model, the constant stress is obtained by considering the ultimate state when $CMOD=CMOD_3$ and the ultimate value of w is considered as $w_u=CMOD_3$.

$$f_{Ftu}=\frac{f_{R3}}{3} \quad (8)$$

The linear model is defined by two reference values, f_{Fts} and f_{Ftu}, which can be obtained by (9) and (10):

$$f_{Fts}=0.45 f_{R1} \quad (9)$$

$$f_{Ftu}=f_{Fts}-\frac{w_u}{CMOD_3}\left(f_{Fts}-0.5 f_{R3}+0.2 f_{R1}\right)\geq 0 \quad (10)$$

These values define a line which, as can be observed in these equations, is based on the experimental values for $CMOD_1$ and $CMOD_3$. Neverheless, the ultimate crack opening w_u is not specifically defined and is kept as the maximum crack opening accepted in structural design, which depends on the ductility required.

Figure 3 shows the schemes for both models: the rigid-plastic and the linear model. It should be noted that while in this figure the linear model shows a load-descending behaviour, depending on the performance of the PFRC, the linear model may present a positive slope which in the MC2010 is referred to as post-crack hardening behaviour.

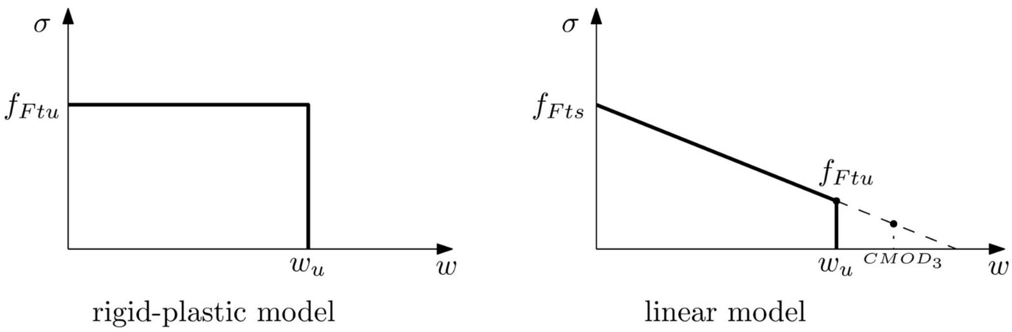

Figure 3: Rigid-plastic model (left) and linear model (right) as described by the MC2010.

2.3. Trilinear model proposed for PFRC

In past papers published by the authors, the behaviour of hardened specimens of self-compacting concrete (SCC) and vibrated conventional concrete (VCC) was studied, with particular examination of how the increase of fibre dosages affects the flexural behaviour of specimens under three-point bending tests [42]. The authors proposed the use of a trilinear softening curve able to reproduce the classical three-point bending tests that develops under pure mode I conditions, as well as a modified version of the test proposed in [43], where cracking initiated under a combination of modes I and II [44].

This trilinear model can be described by three linear parts, as can be seen in Figure **4**. The first linear part reproduces the load decrease due to the failure of the concrete matrix up to the instant at which fibres make a relevant contribution to the specimen flexural strength. The second linear part reproduces the contribution of the fibres up to their maximum tensile capacity and the third part the load decreases due to the final failure of fibres, which can be due to fibre tensile failure or because of the slip of fibres inside the concrete.

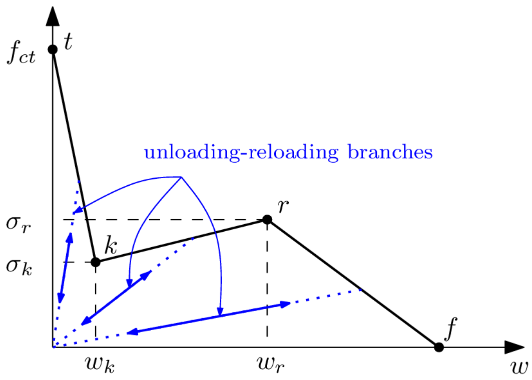

Figure 4: Trilinear diagram proposed by the authors for PFRC.

2.4 Stress-crack opening diagrams used in this study

In order to compare the suitability of each of the three approaches described above, this study examines the experimental behaviour of four PFRC mixes with the numerical predictions of each of them.

The reference experimental results correspond to four PFRC mixes of VCC with four fibre dosages: 3, 4.5, 6 and 10 kg/m^3. The details regarding these experimental works may be consulted in [35, 36].

Regarding the constitutive laws defined by the MC2010, which have been described before, Table 1shows the parameters for each fibre dosage and for each of the two possibilities described in the standard: rigid-plastic model and linear model. Note that the linear model is defined by two points: one for$w=0$ (defined by f_{Fts}) and another one defined by the value of $w=CMOD_3$.

Table 1: Parameters of the rigid-plastic and the linear models for each fibre dosage of PFRC.

	Rigid-plastic model		Linear model		
	f_{Ftu} (MPa)	w_u (mm)	f_{Fts} (MPa)	f_{Ftu} (MPa)	w_u (mm)
PFRC3	0.31	2.5	0.45	0.27	2.5
PFRC4.5	0.49	2.5	0.55	0.48	2.5
PFRC6	0.79	2.5	0.70	0.88	2.5
PFRC10	0.98	2.5	0.88	1.06	2.5

As for the trilinear model, Table 2 shows the coordinates of the points that define them for each fibre dosage. The inverse analysis performed to obtain these values may be consulted in [42].

Table 2: Coordinates of the points that define the trilinear model for each fibre dosage according to the point nomenclature provided in Figure 3.

	T		K		r		f	
	σ (MPa)	w (mm)	σ (MPa)	w (mm)	σ (MPa)	w (mm)	σ (MPa)	w (mm)
PFRC3	3.5	0	0.14	0.12	0.28	2.25	0	7.5
PFRC4.5	3.5	0	0.28	0.09	0.68	2.25	0	7.5
PFRC6	3.5	0	0.43	0.08	1.20	2.25	0	7.5
PFRC10	3.5	0	0.57	0.07	1.45	2.25	0	7.5

Figure 5 shows the diagrams obtained by the three approaches for each fibre dosage. Given that for the linear model the MC2010 does not provide a specific value of w_u, two versions of the model are considered: one with no limit of w_u and another using the $CMOD_3$ as the limit, like in the rigid-plastic model, therefore $w_u = 2.5\,mm$. They will be referred to as "linear model with unlimited development" and "linear model with limited development".

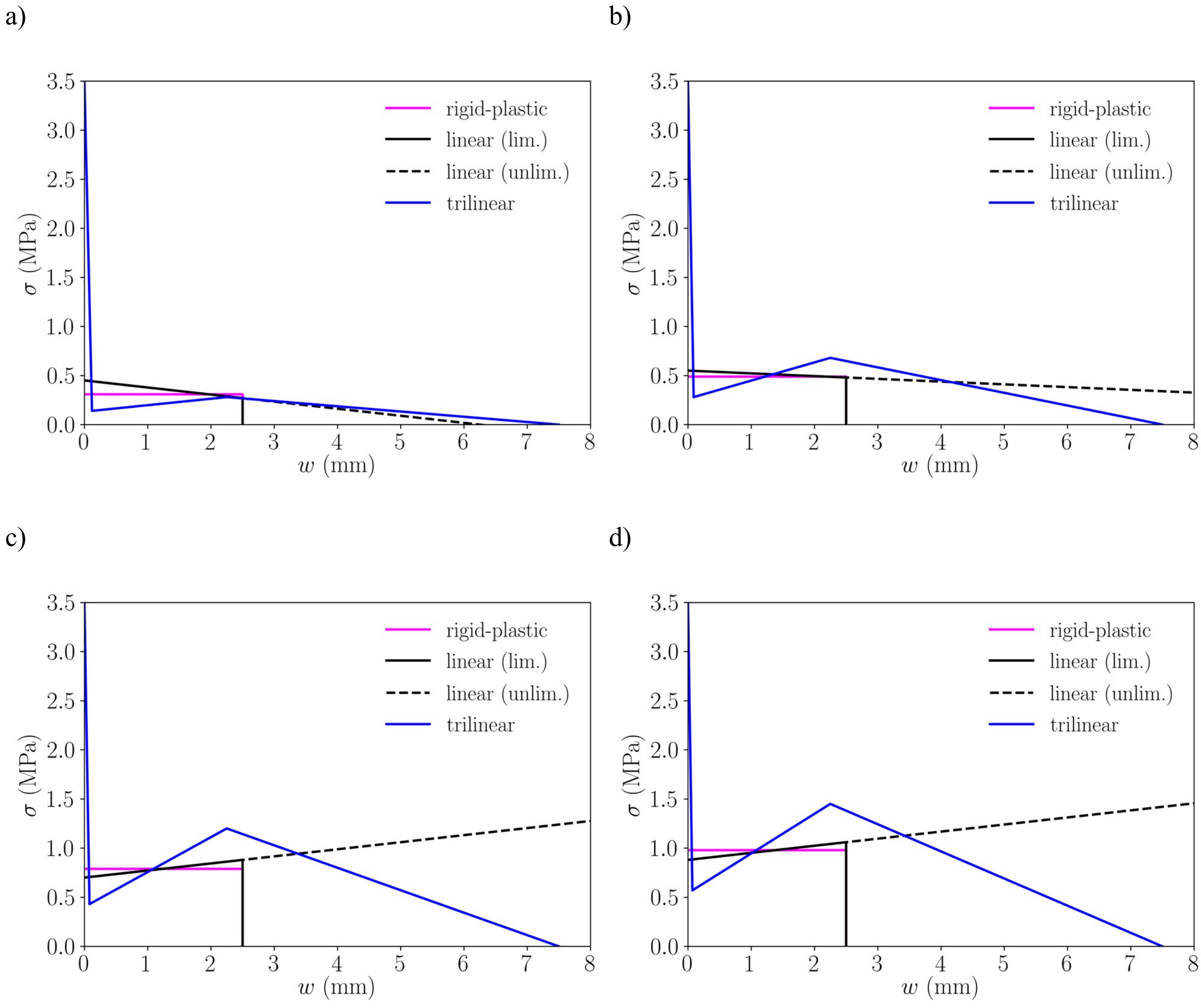

Figure 5: Comparison of the constitutive models obtained by each approach for different fibre dosages: a) 3 kg/m³, b) 4.5 kg/m³, c) 6 kg/m³, d) 10 kg/m³.

3. NUMERICAL SIMULATIONS

The numerical simulations were carried out by means of the finite element method with the commercial software Abaqus®. The softening behaviour was reproduced by the embedded cohesive crack formulation described above, implemented through a user subroutine UMAT in Abaqus. Since, as required by the mathematical formulation described before, only linear triangular elements have been used, and the mesh is refined along the line where cracking develops (see Figure 6a).

In the case of models where fracture is reproduced by a trilinear model and by the linear model of the MC2010 with softening (negative slope of the diagram), all the elements have been modelled by using the same cohesive formulation as that presented before. In the case of those constitutive models with abrupt decrease of strength, like the rigid-plastic model and that termed “linear model with limited development”, convergence issues are usual when employing an implicit integration scheme. The convergence problem in the models that uses “linear softening with unlimited development” with hardening (positive slope of the diagram) provides a different explanation. In these cases, the material becomes harder with increasing values of w, (if an element is damaged it becomes harder, meaning that damage is more likely to develop around it instead of progressing in the element that is already damaged). This leads to an increasing wider region of the specimen that develops, with it being more difficult for the model to find the crack path since, as load displacement increases, there are more possible elements to develop damage which means that convergence is not reached. Figure 6b shows one of these models where damage started developing along the expected crack path but, at some point, started to develop around it and finally convergence was not reached when there were many possible elements to develop damage.

a) b)

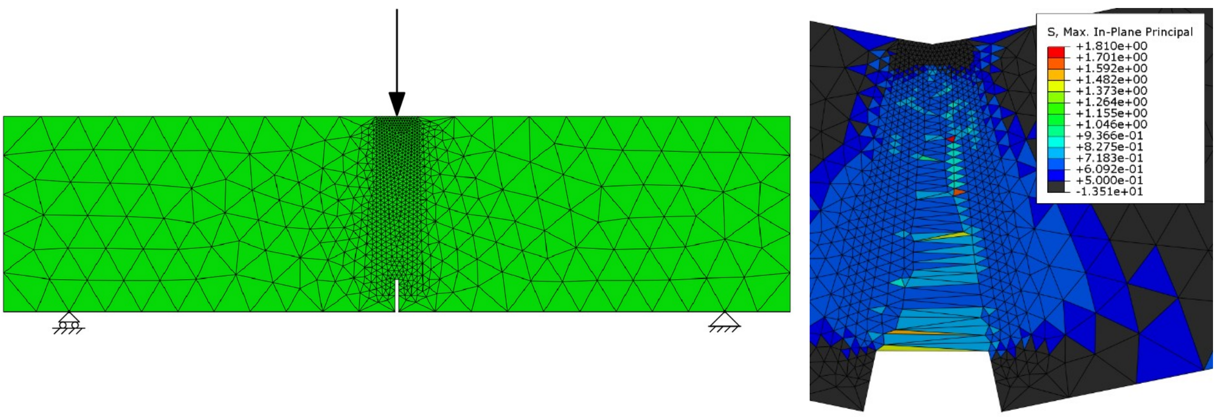

Figure 6: a) Mesh refined along the crack path and boundary conditions, b) Maximum principal stress field in the damaged region of the model that used the linear constitutive law for 6 kg/m³ fibre dosage with no crack tracking. Convergence is not reached.

In such cases with convergence problems, the path of fracture was tracked by defining elements that could be damaged only in the crack path, with the rest of elements behaving elastically.

3.1 Results

Figure 7 shows the load-deflection curves for each of the approaches described for various fibre dosages: 3, 4.5, 6 and 10 kg/m³, therefore reproducing the experimental results of [35, 36].

It is interesting to observe the differences among these approaches. In the case of the rigid-plastic model, diagrams always show a plateau and a subsequent load decrease that describes an exponential-like curve with small load jumps. As these drops are due to the abrupt load decrease described by the rectangular diagram, when an element reaches $w = w_u$, there is a sudden load decrease.

In the case of the “linear model with unlimited development”, the load-deflection diagrams exhibit a linear behaviour after the concrete matrix fails and, depending on the fibre dosage the specimen, may show a softening behaviour (for 3 and 4.5 kg/m^3) or a hardening behaviour (for 6 and 10 kg/m^3). Obviously, in the case of diagrams with hardening this behaviour cannot be realistic, since the load may increase without a limit. Nevertheless, it is interesting to compare these results with those of the linear model with limited development that display an analogous behaviour until the most damaged element reaches $w = w_u$, when the load-deflection diagrams show a highly similar behaviour to that observed with the rigid-plastic model. In all cases, the load drop follows an exponential-like shape with small jumps that can be explained as for the rigid-plastic model.

Lastly, if the results obtained with a trilinear model are observed, remarkable differences can be highlighted compared with any of the results obtained with the other approaches. Firstly, the maximum load reached that identifies the beginning of the fracture process is higher than in any of the other cases and the shape shows an initial load decay, followed by a load recovery and another load decay later. Secondly, the last load decay, which identifies the last part of the test until failure, shows a curved shape that has the opposite curvature if compared with results obtained with the rigid-plastic model and the linear model with limited development.

a)

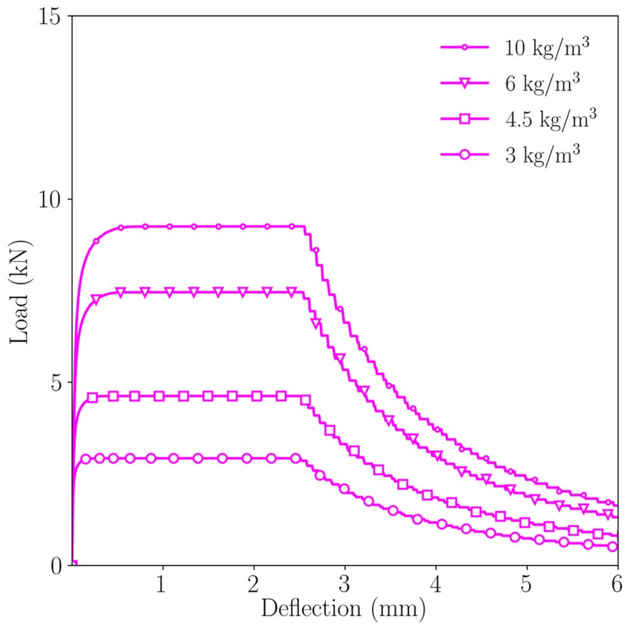

b)

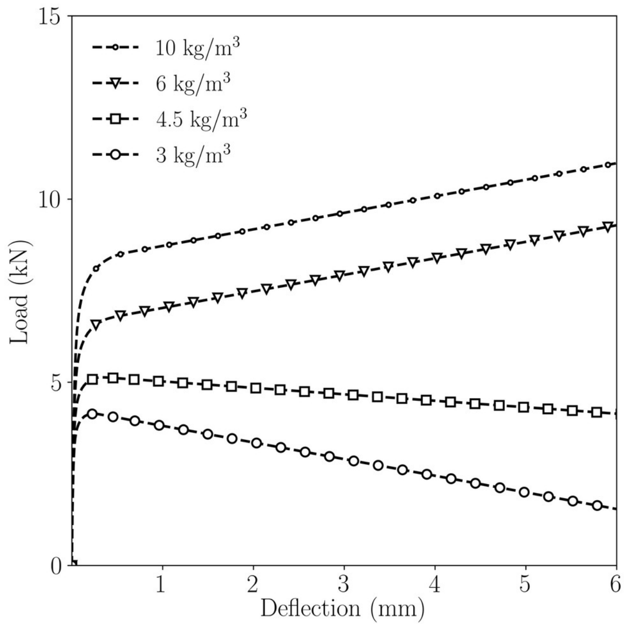

c)

d)

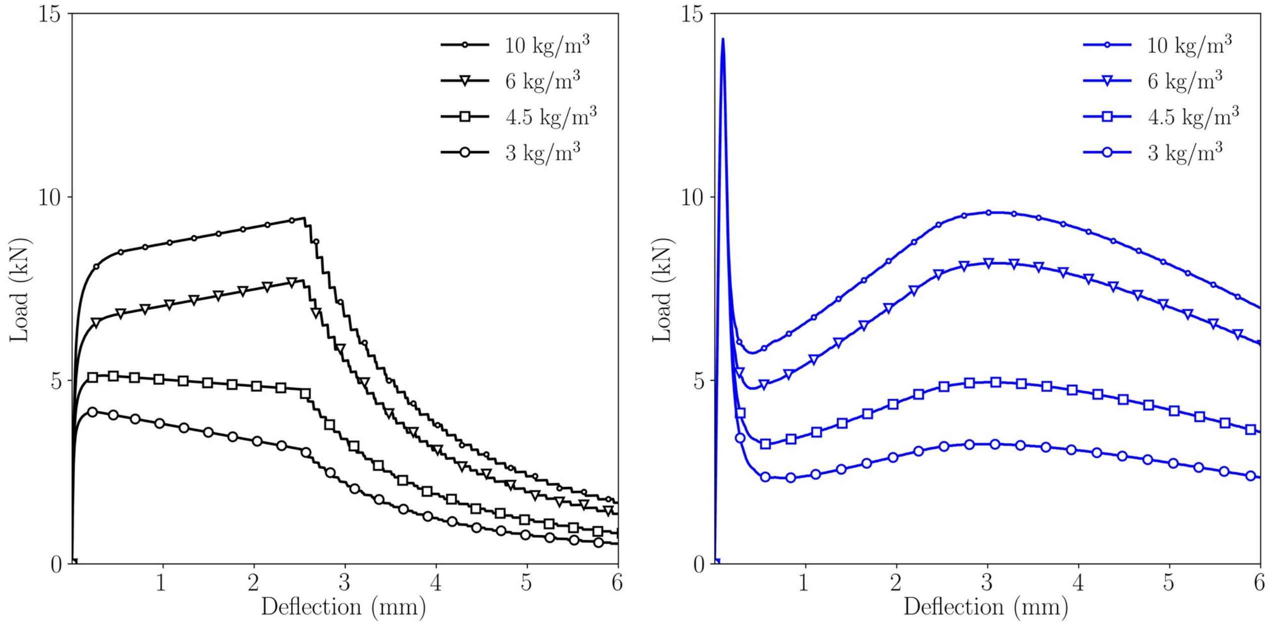

Figure 7: Comparison of the load-deflection diagram obtained with each approach for different fibre dosages: a) rigid-plastic model, b) linear elastic model (unlimited development), c) linear elastic model (limited development), d) trilinear model.

4. DISCUSSION

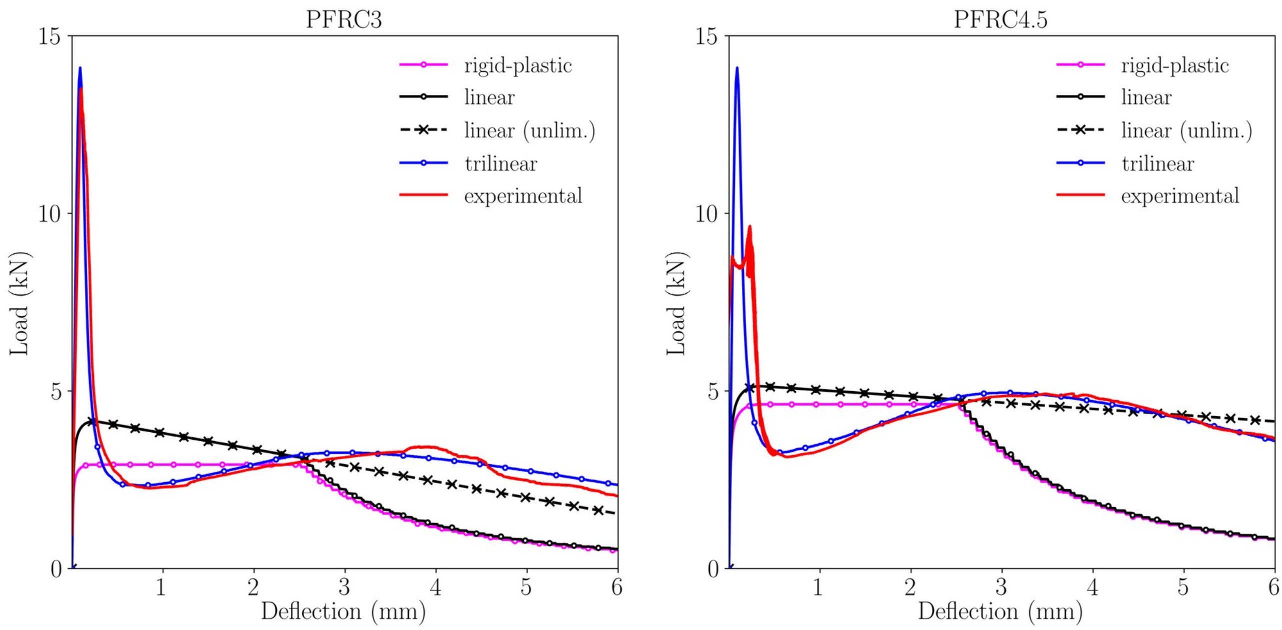

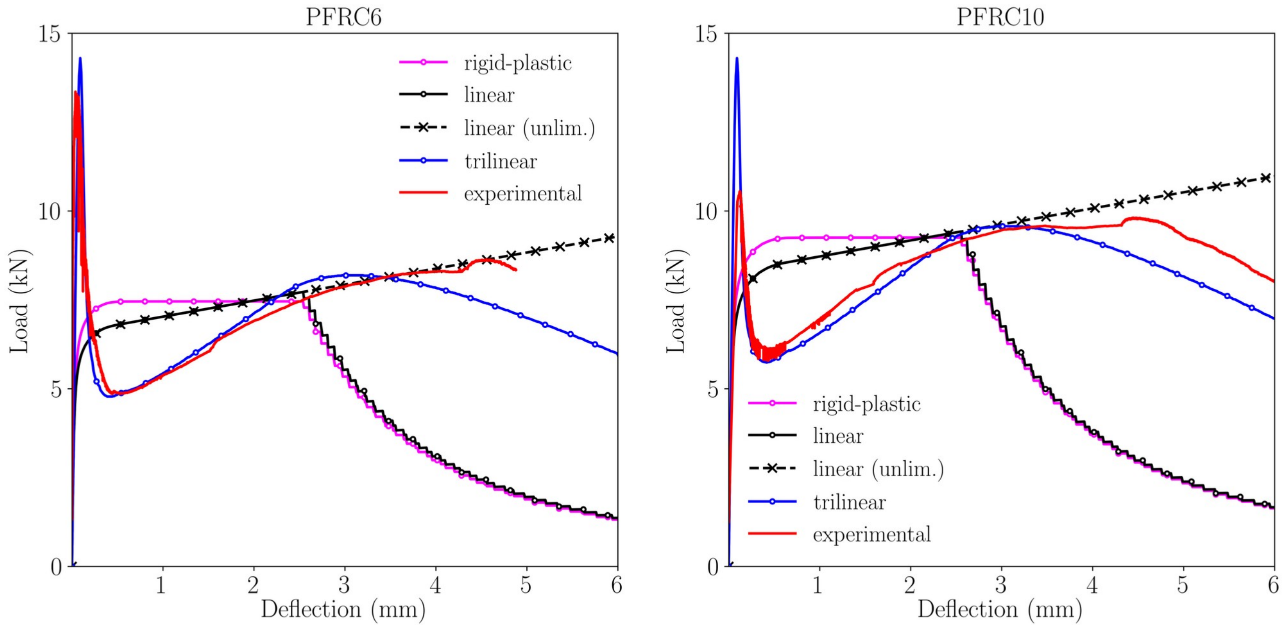

Figure 8. Comparison among the experimental curves and the simulations results obtained with the constitutive models implemented.

In Figure 8 it can be seen that in the case of PFRC3 there are remarkable changes in the shape of the curves obtained through using the post-peak constitutive functions analysed. Regarding the rigid-plastic model and the linear model proposed by the MC2010, none is capable of reproducing the peak load registered in the experimental tests (it should be taken into account that usually 3kg/m^3 of polyolefin fibres do not allow PFRC to be classified as structural concrete). However, the trilinear approach accurately captures such a peak load. This phenomenon might be explained because the trilinear approach is the only one that establishes a progressive unloading after reaching peak load. Similarly, the trilinear approach is able to simulate the unloading process of the PFRC3 formulation. In the case of the rigid-plastic approach, when the deflection increases the load-deflection curve features a plateau. This stretch ends when a deflection of 3mm is reached. From that deflection onwards, a progressive unloading takes place which does not fit the experimental behaviour. In the case of the “linear approach (unlimited)”, as the slope is negative the load decreases as the deflection increases. Consequently, such simulation is able to maintain its load-bearing capacity beyond 6mm of deflection. The results obtained with the “linear model (limited)” softening curve also boast a descending slope until a progressive unloading starts at 3mm of deflection. From that point onwards, the curve is not capable of reproducing the experimental behaviour. It should be underlined that the rigid-plastic approach and both linear approaches obtain load-deflection curves that are above the experimental one until a deflection of 2.5mm is reached. For greater deflections, the experimental curve is above that predicted by both linear approaches. In the case of the rigid-plastic model, a similar comment could be made. However, in the case of the trilinear approach a close reproduction of the experimental behaviour PFRC3 is achieved throughout the test.

In the part of Figure 8 that corresponds to PFRC4.5, it may be observed that the differences perceived in the curves related with PFRC3 still appear. The peak load, as in the previous case, is not captured by any approach proposed by the MC2010 or even the modification proposed for the linear model. However, the trilinear constitutive model is able to simulate the flexural tensile behaviour of the material prior to the development of the failure surface. As in the case of PFRC3, the trilinear softening function was able to simulate the experimental behaviour of the PFRC4.5 in all its stages. Regarding the behaviour of the rigid-plastic model, it may be seen that its main feature is a constant load bearing capacity until a 3mm deflection is reached. From that point onwards the rigid-plastic model is below the experimental curve. As regards to both linear approaches are above the experimental curve between 0.5 and 2.5mm of deflection. There are few differences between the rigid-plastic approach and the linear approach because the slope of the linear model is close to zero. One feature that could be highlighted is that the unlimited linear model behaviour is close to the experimental one for deflections between 2.5 and 6mm.

Regarding the curves shown for PFRC6, a similar trend may be perceived if the experimental curve is compared with the one obtained with the rigid-plastic approach. For deflections ranging from 0.3mm to 2.5mm, the simulated curve is above the experimental one as the plateau is close to the experimental maximum post-peak load. From 2.5mm of deflection, the unloading branch of the rigid-plastic model features a steep degree of unloading that is below the experimental behaviour. Regarding the linear model with the unlimited option, it should be pointed out that as the slope of the load-deflection curve is positive, the model is not able to capture the material failure as its load bearing capacity increases with deflection. Thus, beyond 3.5 mm of deflection the linear model is above the experimental curve. This also occurs between 0.3mm and 2.5mm of deflection. If the limited linear model is studied, similar comments to those previously mentioned regarding its unlimited version could be made until 2.5mm of deflection is reached. From greater deflection values there are remarkable differences between the behaviour of the model and the real one because steep unloading appears in the simulated curve. As regards the simulation performed with the trilinear approach, it could be said that it is able to reproduce the shape and values of the experimental curves although there are certain differences from 3.5mm onwards. In this case, the experimental behaviour is slightly above the simulated one.

Regarding PFRC10, similar features to those observed in PFRC6 can be seen. The rigid-plastic approach has similar characteristics than those previously mentioned in the case of PFRC6. A similar trend may be mentioned when the differences between the experimental curve and both linear approaches are evaluated. On this occasion, the slope of the linear model is positive and no failure of the material occurs. If the model is limited a under evaluation of the behaviour of PFRC10 is observed. Regarding the trilinear approach, for deflection values greater than the maximum post-peak load such a curve marginally underestimates the load-bearing capacity of the material.

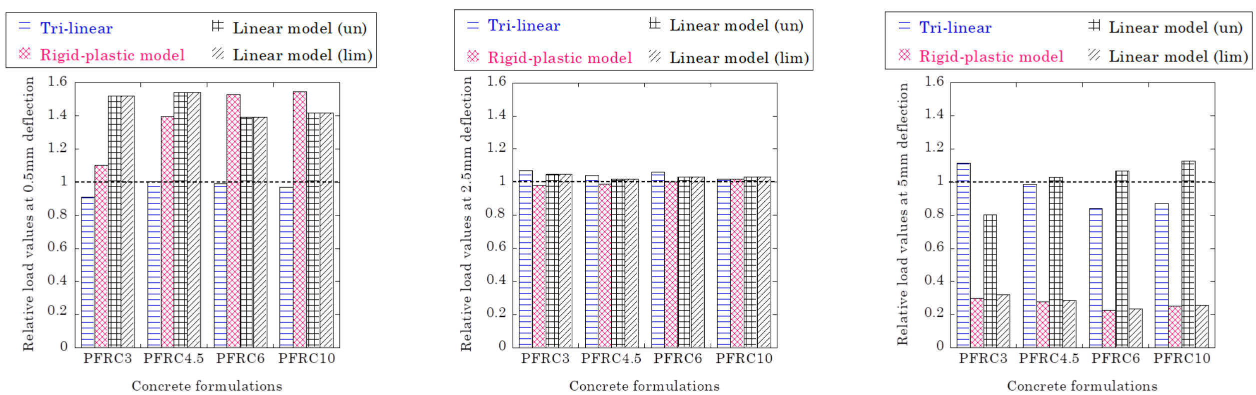

Figure 9. Comparison of the loads borne by the simulations at certain deflection values with respect to the experimental values.

Figure 9 provides a comparison among the loads registered at different deflection values in the simulations performed and takes into account the three constitutive models studied. The values shown are relative to the value obtained in the experimental test which is considered as unity. Consequently, if a load value obtained in the simulation is greater than the one obtained in the test the column that appears in Figure 9 is greater than one. On the contrary, values lower than the unity reflect that the simulation underestimates the real load-bearing capacity of the material. Such load analysis has been performed at three deflections: 0.5mm, 2.5mm and 5mm. The values of deflection studied are based on the almost linear relation that exists between the crack width and the deflection. Consequently, it may be considered that a deflection value of 0.5mm is close to the crack width used for checking the SLS of the structural element. Correspondingly, the deflection value of 2.5mm has been chosen because such a value is close to the crack width chosen when analysing the ultimate limit state of the structural element. Lastly, regarding the 5mm of deflection, such a value has been chosen as it may reflect the suitability of the constitutive models to detect the ultimate bearing capacity of the material at great deflections.

When the analysis of the SLS is performed for the PFRC formulations, several relevant features are evident. In the case of PFRC3, it may be seen that while the trilinear approach underestimates the capacity of the material, the two proposals of the MC2010 boast loads greater than the experimental one. In the case of the linear model, both versions obtain a load approximately 1.6 times the experimental one. In the case of the rigid-plastic model, although it also overestimates the experimental value registered, it is much closer to the real one. In the case of PFRC4.5, all the values obtained in the simulations are greater than the experimental ones (except the trilinear one which is much closer to the real value). On this occasion, the load values of the rigid-plastic model are close to those obtained with the linear models. Similar results were obtained for the PFRC6 and PFRC10 formulations.

These features seem to be a consequence of the load-crack mouth opening displacement curve taken as reference to set the requirements needed for considering the contribution of fibres in FRC (see Figure 2a). As such a reference curve boasted an f_{R3} value lower than f_{R1} if the design values are obtained by reducing the load obtained in f_{R3}, such a constitutive model might have an accurate correlation with material behaviour. Nevertheless, in the case of PFRC, given that the value of f_{R3} is greater than f_{R1}, the design value obtained for reduced strains might not be an accurate reproduction of the experimental behaviour.

When analysing the ULS, similar to the behaviour that appears at 2.5mm of deflection, it may be seen that the trilinear approach and those proposed by the MC2010 reflect with a notable degree of accuracy the experimental behaviour of the material.

Regarding the loads obtained with the trilinear approach, all load values are within a 20% margin from the experimental at 5mm of deflection. In the case of the rigid-plastic model and the limited linear model, both are far from the experimental results for any fibre dosage. In the case of the unlimited linear model, the load values are below the experimental ones when the slope is negative. On the contrary, when the slope is positive such values are slightly above those registered in the tests.

Table 3. Fracture energy consumption in the experimental tests and in the simulations.

Fracture energy

	Experimental	**Trilinear**		**Rigid-plastic model**		**Linear model (un.)**		**Linear model (lim.)**	
PFRC3	G_F(N/mm)	G_F (N/mm)	Δ(%)	G_F (N/mm)	Δ(%)	G_F (N/mm)	Δ(%)	G_F (N/mm)	Δ(%)
0.5 mm	0.160	0.147	-7.99	0.076	-52.55	0.106	-33.47	0.106	-33.47
2.5 mm	0.435	0.433	-0.60	0.387	-11.07	0.486	11.63	0.486	11.63
5 mm	0.849	0.846	-0.28	0.585	-31.07	0.829	-2.31	0.698	-17.75

	Experimental	**Trilinear**		**Rigid-plastic model**		**Linear model (un.)**		**Linear model (lim.)**	
PFRC4.5	G_F(N/mm)	G_F (N/mm)	Δ(%)	G_F (N/mm)	Δ(%)	G_F (N/mm)	Δ(%)	G_F (N/mm)	Δ(%)
0.5 mm	0.199	0.160	-19.68	0.118	-40.63	0.131	-34.23	0.131	-34.23
2.5 mm	0.609	0.582	-4.47	0.610	0.14	0.657	7.88	0.657	7.88

5 mm	1.239	1.210	-2.34	0.924	-25.43	1.262	1.83	0.978	-21.06

	Experimental	**Trilinear**		**Rigid-plastic model**		**Linear model (un.)**		**Linear model (lim.)**	
PFRC6	G_F(N/mm)	G_F (N/mm)	Δ(%)	G_F (N/mm)	Δ(%)	G_F (N/mm)	Δ(%)	G_F (N/mm)	Δ(%)
0.5 mm	0.196	0.176	-9.91	0.181	-7.42	0.164	-16.04	0.164	-16.04
2.5 mm	0.849	0.849	-0.04	0.979	15.34	0.941	10.88	0.941	10.88
5 mm	1.937	1.892	-2.33	1.488	-23.18	2.045	5.58	1.470	-24.11

	Experimental	**Trilinear**		**Rigid-plastic model**		**Linear model (un.)**		**Linear model (lim.)**	
PFRC10	G_F(N/mm)	G_F (N/mm)	Δ(%)	G_F (N/mm)	Δ(%)	G_F (N/mm)	Δ(%)	G_F (N/mm)	Δ(%)
0.5 mm	0.184	0.193	5.22	0.221	20.24	0.202	10.23	0.202	10.23
2.5 mm	1.016	0.994	-2.10	1.206	18.69	1.155	13.76	1.155	13.76
5 mm	2.288	2.212	-3.33	1.844	-19.42	2.485	8.59	1.808	-21.01

Another material property that might be of interest is the fracture energy required to generate certain deflections of the concrete element. Consequently, the fracture energy at the aforementioned deflections has been obtained for all the concrete formulations and constitutive models analysed. Such results can be seen in Table 3, where the variation of the fracture energy of the curves obtained in the simulations performed by using the constitutive models implemented has been related to that obtained in the experimental tests.

In the case of the trilinear model, it can be seen that a notable precision was obtained at all the deflections analysed. Regarding the rigid-plastic model, there was a certain degree of scattering between the values obtained at 0.5mm between the experimental values and the simulated ones. Such scattering was reduced at 2.5mm of deflection and increased at 5mm of deflection. In the case of the linear model, the accuracy of the prediction of the fracture energy absorbed by the material increased as the deflection grew. In Table 3 it may be seen that the proposed limitation of the linear approach did not enhance the accuracy of the prediction of the fracture energy absorbed.

5. CONCLUSIONS

The present contribution has been developed by implementing the constitutive relations proposed by the MC2010 for FRC in a user material subroutine. With such implementations, a series of experimental three-point bending fracture tests have been simulated seeking to assess the adaptability of these constitutive relations to PFRC. In addition, a trilinear model and an unlimited version of the linear model proposed by MC2010 have been employed as comparisons.

The simulations carried out with the implementation of the trilinear softening function proposed by the authors showed a remarkable resemblance with the experimental behaviour of PFRC. Regarding the simulations performed through using the constitutive models proposed by MC2010, it was observed that they might not replicate the flexural behaviour of PFRC precisely. Neither the peak load nor the unloading process appeared in the simulations performed with the rigid-plastic and linear constitutive relations. This might be due to the absence of a softening stretch after reaching the tensile strength of the material. For reduced strains, the material models of MC2010 boast a greater load-bearing capacity than the experimental results of [35,36]. On the contrary, there is an accurate correlation between simulations and the experimental results at ULS. For deflections greater than 3 mm, the rigid-plastic model and the limited linear model boast a drastic unload that does not reproduce the experimental behaviour of any formulation. In the cases of PFRC6 and PFRC10, the positive slope of the unlimited linear model implies an infinite load bearing capacity. Such a feature might be noted in order to avoid risks when structural designing.

When analysing the load values obtained at 0.5mm of deflection, it is seen that the constitutive relations proposed by the MC2010 are above the experimental results. However, the trilinear model suggested by the authors assesses accurately the material properties at this deflection value. At ULS, the relations proposed by the MC2010 and that proposed by the authors are able to reproduce with notable exactness the experimental load values. Regarding the ultimate load-bearing capacity of the material, which was assumed at a deflection of 5mm, both the trilinear and unlimited linear model were close to the load-bearing capacity of the material. On the contrary, the rigid-plastic model and the limited version of the linear model clearly underestimated the mechanical properties of PFRC.

Regarding the study of the fracture energy performed, it should be stated that the trilinear constitutive model achieves the greatest degree of accuracy in all the deformation states analysed. In the case of the constitutive relations proposed by the MC2010, it should be mentioned that they became more precise as the fibre dosage grew. For high displacements, the amount of energy absorbed when using the rigid-plastic or linear relation was closer to the real ones as a general trend.

Based on the aforementioned arguments, it seems that the rigid-plastic and the linear models proposed by the MC2010 might be employed with caution at SLS when applied to PFRC. This might be a result of the idealisation of the FRC fracture bending behaviour considered in MC2010. Such idealisation might offer a limited degree of accuracy when applied to FRC formulations where f_{R3} is notably greater than f_{R1}. The authors consider that if the results of the EN-14651 fracture tests boast a clear three-stretch behaviour after reaching the peak load (unloading-reloading-final unloading), a trilinear constitutive relation might be adopted as an alternative to the models proposed by MC2010. This is relevant given that the latter models were developed considering that steel fibres were the main option for reinforcing concrete with fibres.

6. ACKNOWLEDGEMENTS

The authors gratefully acknowledge the financial support provided by the Ministry of Economy and Competitiveness of Spain by means of the Research Fund Project PID2019-108978RB-C31R. They also offer their gratitude to SIKA SAU for supporting the Enterprise University Chair “Cátedra Sika-UPM”.

References

[1] M. S. Low, Material flow analysis of concrete in the United States, Doctoral dissertation, Massachusetts Institute of Technology, 2005.

[2] E. Davidson, “Defining the trend: Cement consumption versus Gross Domestic Product,” *Global Cement Magazine,* vol. June, pp. 8-14, 2014.

[3] M. S. Imbabi, C. Carrigan and S. McKenna, “Trends and developments in green cement and concrete technology,” *International Journal of Sustainable Built Environment,* vol. 1, no. 2, pp. 194-216, 2012.

[4] S. S. Bhattacharjee and P. Leger, “Seismic cracking and energy dissipation in concrete gravity dams.,” *Earthquake Engineering & Structural Dynamics,* vol. 22, no. 11, pp. 991-1007, 1993.

[5] M. Briffaut, F. Benboudjema, J. M. Torrenti and G. Nahas, “Effects of early-age thermal behaviour on damage risks in massive concrete structures,” *European Journal of Environmental and Civil Engineering,* vol. 16, no. 5, pp. 589-605, 2012.

[6] S. M. Abdelkader, E. R. Pozo and A. M. Terrades, “Evolution of microstructure and mechanical behavior of concretes utilized in marine environments,” *Materials & Design,* vol. 31, no. 7, pp. 3412-3418, 2010.

[7] A. Steffens, D. Dinkler and H. Ahrens, “Modeling carbonation for corrosion risk prediction of concrete structures,” *Cement and Concrete Research,* vol. 32, no. 6, pp. 935-941, 2002.

[8] M. Alexander, A. Bertron and N. De Belie, Performance of cement-based materials in aggressive aqueous environments, Berlin: Springer, 2013.

[9] F. P. Glasser, J. Marchand and E. Samson, “Durability of concrete — Degradation phenomena involving detrimental chemical reaction,” *Cement and Concrete Research,* vol. 38, no. 2, pp. 226-246, 2008.

[10] J. Wongpa, K. Kiattikomol, C. Jaturapitakkul and P. Chindaprasirt, “Compressive strength, modulus of elasticity, and water permeability of inorganic polymer concrete,” *Materials & Design,* vol. 31, no. 10, pp. 4748-4754, 2010.

[11] F. P. Zhou, F. D. Lydon and B. I. G. Barr, “Effect of coarse aggregate on elastic modulus and compressive strength of high performance concrete,” *Cement and concrete research,* vol. 25, no. 1, pp. 177-186, 1995.

[12] T. Nishikawa, J. Yoshida, T. Sugiyama and Y. Fujino, “Concrete crack detection by multiple sequential image filtering. Computer-Aided Civil and Infrastructure Engineering,” *2012,* vol. 27, no. 1, pp. 29-47.

[13] S. Park, S. Ahmad, C. B. Yun and Y. Roh, “Multiple crack detection of concrete structures using impedance-based structural health monitoring techniques,” *Experimental Mechanics,* vol. 46, no. 5, pp. 609-618, 2006.

[14] M. G. Alberti, A. Enfedaque and J. C. Gálvez, “On the mechanical properties and fracture behavior of polyolefin fiber-reinforced self-compacting concrete,” *Construction and Building Materials,* vol. Volume 55, pp. 274-288, 2014.

[15] M. G. Alberti, A. Enfedaque, J. C. Gálvez and V. Agrawal, “Fibre distribution and orientation of macro-synthetic polyolefin fibre reinforced concrete elements.,” *Construction and Building Materials, ,* vol. 122, pp. 505-517, 2016.

[16] B. Belletti, R. Cerioni, A. Meda and G. Plizzari, “Design aspects on steel fiber-reinforced concrete pavements,” *Journal of Materials in Civil Engineering,* vol. 20, no. 9, pp. 599-607, 2008.

[17] C. Achilleos, D. Hadjimitsis, K. Neocleous, K. Pilakoutas, P. O. Neophytou and S. Kallis, “Proportioning of steel fibre reinforced concrete mixes for pavement construction and their impact on environment and cost,” *Sustainability,* vol. 3, no. 7, pp. 965-983, 2011.

[18] N. Buratti, B. Ferracuti and M. Savoia, “Concrete crack reduction in tunnel linings by steel fibre-reinforced concretes,” *Construction and Building Materials,* vol. 44, pp. 249-259, 2013.

[19] T. Kasper, C. Edvardsen, G. Wittneben and D. Neumann, “Lining design for the district heating tunnel in Copenhagen with steel fibre reinforced concrete segments,” *Tunnelling and Underground Space Technology,* vol. 23, no. 5, pp. 574-587, 2008.

[20] F. Germano, G. Tiberti and G. Plizzari, “Post-peak fatigue performance of steel fiber reinforced concrete under flexure,” *Materials and Structures,* vol. 49, no. 10, pp. 4229-4245, 2016.

[21] D. Y. Yoo and N. Banthia, “Mechanical and structural behaviors of ultra-high-performance fiber-reinforced concrete subjected to impact and blast,” *Construction and Building Materials,* vol. 149, pp. 416-431, 2017.

[22] G. T. Halvorsen, C. E. Kesler, A. R. Robinson and J. A. Stout, Durability and Physical Properties of Steel Fiber Reinforced Concrete, 1976.

[23] V. Marcos-Meson, G. Fischer, C. Edvardsen, T. Skovhus and A. Michel, “Durability of Steel Fibre Reinforced Concrete (SFRC) exposed to acid attack – A literature review,” *Construction and Building Materials,* vol. 200, pp. 90-501, 2019.

[24] B. Berge, The ecology of building materials, Routledge, 2009.

[25] M. G. Alberti, A. Enfedaque, J. C. Gálvez and L. Pinillos, “Structural Cast-in-Place Application of Polyolefin Fiber–Reinforced Concrete in a Water Pipeline Supporting Elements,” *Journal of Pipeline Systems Engineering and Practice,* vol. 8(4), 2017.

[26] K. Behfarnia and A. Behravan, “Application of high performance polypropylene fibers in concrete lining of water tunnels,” *Materials & Design,* vol. 55, pp. 274-279, 2014.

[27] H. B. Poorsaheli, A. Behravan, S. T. T. Aghda and A. Gholami, “A study on the durability parameters of concrete structures reinforced with synthetic fibers in high chloride concentrated shorelines,” *Construction and Building Materials,* vol. 200, pp. 578-585, 2019.

[28] B. Chiaia, A. P. Fantilli and P. Vallini, “Combining fiber-reinforced concrete with traditional reinforcement in tunnel linings,” *Engineering Structures,* vol. 31, no. 7, pp. 1600-1606, 2009.

[29] Sweden Standard SS812310: 2014 Fibre Concrete, “Design of Fibre Concrete Structures”.

[30] China CECS38:2004, “Technical Specification for Fiber Reinforced Concrete Structures provides guidelines for various applications”.

[31] DBV, “Technologie des Stahlfaser-betons und Stahlfaserprit,” 1992.

[32] CNR-DT 204, “Guide for the design and construction of fiber-reinforced concrete structures,” Consiglio Nazionale delle Riserche, Roma, 2006.

[33] EHE-08, Spanish Structural Concrete Code, Spanish Minister of Public Works, 2008.

[34] India - ICI – G 501, “Guidelines for Selection, Specification & Acceptance of fiber and fiber concrete”.

[35] M. G. Alberti, A. Enfedaque, J. C. Gálvez and V. Agrawal, “Reliability of polyolefin fibre reinforced concrete beyond laboratory sizes and construction procedures,” *Composite Structures,* vol. 140(15), pp. 506-524, 2016.

[36] M. G. Alberti, A. Enfedaque and J. C. Gálvez, “Comparison between polyolefin fibre reinforced vibrated conventional concrete and self-compacting concrete,” *Construction & Building Materials,* vol. 85(15), pp. 182-194, 2015.

[37] EN 14651:2007+A1, Test method for metallic fibre concrete. Measuring the flexural tensile strength (limit of proportionality (LOP), residual), 2007.

[38] fib Model Code, Model Code, Paris: Fédération Internationale du Béton fib/International Federation for Structural Concrete, 2010.

[39] A. Hillerborg, M. Modéer and P. E. Petersson, “Analysis of crack formation and crack growth in concrete by means of fracture mechanics and finite elements,” *Cement and Concrete Research,* vol. 6(6), pp. 773-78, 1976.

[40] J. Sancho, J. Planas, D. Cendón, E. Reyes and J.C. Gálvez, “An embedded crack model for finite element analysis of concrete fracture,” *Engineering Fracture Mechanics,* vol. 74, no. 1, pp. 75-86, 2007.

[41] E. Reyes, J. C. Gálvez, M. J. Casati, D. Cendón, J. Sancho and J. Planas, "An embedded cohesive crack model for finite element analysis of brickwork masonry fracture," *Engineering Fracture Mechanics,* vol. 76, no. 12, pp. 1930-1944, 2009.

[42] M. G. Alberti, A. Enfedaque, J. C. Gálvez and E. Reyes, "Numerical modelling of the fracture of polyolefin fibre reinforced concrete by using a cohesive fracture approach.," *Composites Part B: Engineering,* vol. 111, pp. 200-210, 2017.

[43] J. C. Gálvez, M. Elices, G. Guinea and J. Planas, "Mixed mode fracture of concrete under proportional and nonproportional loading," *International Journal of Fracture,* vol. 94, no. 3, pp. 267-284, 1998.

[44] F. Suárez, J. C. Gálvez, A. Enfedaque and M. G. Alberti, "Modelling fracture on polyolefin fibre reinforced concrete specimens subjected to mixed-mode loading," *Engineering Fracture Mechanics,* vol. 211, pp. 244-253, 2019.